

# Enhancement effect of mass imbalance on Fulde-Ferrell-Larkin-Ovchinnikov type of pairing in Fermi-Fermi mixtures of ultracold quantum gases

Jibiao Wang, Yanming Che, Leifeng Zhang and Qijin Chen\*

Department of Physics and Zhejiang Institute of Modern Physics, Zhejiang University, Hangzhou, Zhejiang 310027, China and Synergetic Innovation Center of Quantum Information and Quantum Physics, Hefei, Anhui 230026, China

(Dated: March 1, 2022)

Ultracold two-component Fermi gases with a tunable population imbalance have provided an excellent opportunity for studying the exotic Fulde-Ferrell-Larkin-Ovchinnikov (FFLO) states, which have been of great interest in condensed matter physics. However, the FFLO states have not been observed experimentally in Fermi gases in three dimensions (3D), possibly due to their small phase space volume and extremely low temperature required for an equal-mass Fermi gas. Here we explore possible effects of mass imbalance, mainly in a  ${}^6\text{Li}$ - ${}^{40}\text{K}$  mixture, on the one-plane-wave FFLO phases for a 3D homogeneous case at the mean-field level. We present various phase diagrams related to the FFLO states at both zero and finite temperatures, throughout the BCS-BEC crossover, and show that a large mass ratio may enhance substantially FFLO type of pairing.

The past decade has seen great progress in ultracold atomic Fermi gas studies [1, 2]. With the easy tunability in terms of interaction, dimensionality, population imbalance as well as mass imbalance [1, 2], ultracold Fermi gases have provided a good opportunity to study many exotic quantum phenomena. In particular, the Fulde-Ferrell-Larkin-Ovchinnikov (FFLO) states, which were first predicted by Fulde and Ferrell [3] (FF) and Larkin and Ovchinnikov [4] (LO) in an  $s$ -wave superconductor in the presence of a Zeeman field about fifty years ago, have attracted enormous attention in condensed matter physics [5], including heavy-fermion [6], organic [7] and high  $T_c$  superconductors [8], nuclear matter [9] and color superconductivity [10], and ultracold Fermi gases [11]. In these exotic states, Cooper pairs condense at a finite momentum  $\mathbf{q}$ , with an order parameter of the form of either a plane-wave  $\Delta(\mathbf{r}) = \Delta_0 e^{i\mathbf{q}\cdot\mathbf{r}}$  or a standing wave  $\Delta(\mathbf{r}) = \Delta_0 \cos(\mathbf{q}\cdot\mathbf{r})$  for the FF and LO states, respectively. Despite many theoretical studies on the FFLO states in equal-mass Fermi gases, both in a 3D homogeneous case [12, 13] and in a trap [14–16], the experimental search for these exotic states in atomic Fermi gases still has not been successful [17, 18], largely because they exist only in a *small* region at *very low* temperature in the phase space [12, 15]. To find these elusive states, attention has been paid to more complex systems. There have been theoretical investigations in either Fermi-Fermi mixtures [19, 20] or equal-mass Fermi gases with spin-orbit coupling [21, 22] or in an optical lattice [23]. Recently, Stoof and coworkers [19] found an instability toward a supersolid state [24] in a homogeneous  ${}^6\text{Li}$ - ${}^{40}\text{K}$  mixture in the unitarity and BCS regimes. Using a mean-field theory and the Bogoliubov–de Gennes (BdG) formalism, they have also studied the LO states for the unitary case [20]. However, it is hard to perform stability analysis for various phases in the BdG formalism. Other types of mass-imbalanced systems such as the  ${}^6\text{Li}$ - ${}^{173}\text{Yb}$  mixture were not considered in Ref. [20].

In this paper, we will investigate the *one-plane-wave* FFLO states (i.e., the FF states) in a homogeneous  ${}^6\text{Li}$ - ${}^{40}\text{K}$  mixture, as well as for other mass ratios, as they undergo BCS–BEC crossover, using a mean-field theory. We will present several

$T$ - $p$  (where  $p$  is the population imbalance) phase diagrams to show the FFLO regions under typical interaction strengths ( $1/k_F a$ ) at finite temperature, as well as  $p$ - $1/k_F a$  phase diagrams at zero temperature. We find that when the heavy species,  ${}^{40}\text{K}$ , is the majority, an  $s$ -wave FFLO phase, which is stable against phase separation, persists throughout the BCS through BEC regimes, with the population imbalance evolving from small to large. In contrast, when the light species,  ${}^6\text{Li}$ , is the majority, such an FFLO phase exists only in the BCS regime. At unitarity, the phase space of FFLO states becomes substantially enlarged as the mass ratio increases. The superfluid transition temperature  $T_c$  of the FFLO states may be enhanced by a factor of about 3 and 7 for a large mass ratio as in  ${}^6\text{Li}$ - ${}^{40}\text{K}$  [25] and  ${}^6\text{Li}$ - ${}^{173}\text{Yb}$  [26, 27], respectively, in comparison with the equal-mass case [12], which is hardly accessible experimentally [17]. Therefore, one may find it realistic to experimentally observe the exotic FFLO states in unitary ultracold Fermi-Fermi mixtures with a large mass ratio.

We also find that at zero temperature the phase space of stable FFLO states becomes larger as the mass ratio increases. This has never been reported by other previous works.

We consider a three-dimensional (3D) Fermi-Fermi mixture with a short-range contact potential of strength  $U < 0$ , where momentum  $\mathbf{k}$  pairs with  $\mathbf{q} - \mathbf{k}$  and thus Cooper pairs have a nonzero center-of-mass momentum  $\mathbf{q}$ . The dispersion of free atoms is given by  $\xi_{\mathbf{k},\sigma} = \mathbf{k}^2/2m_\sigma - \mu_\sigma$ , where  $m_\sigma$  and  $\mu_\sigma$  are the mass and chemical potential for (pseudo)spin  $\sigma = \uparrow, \downarrow$ , respectively. We set the volume  $V = 1$ , and  $\hbar = k_B = 1$ . At the mean-field level, the system with a one-plane wave LOFF solution can be described by the following Hamiltonian

$$H^{MF} = \sum_{\mathbf{k},\sigma} \xi_{\mathbf{k},\sigma} c_{\mathbf{k},\sigma}^\dagger c_{\mathbf{k},\sigma} - \sum_{\mathbf{k}} (\Delta c_{\mathbf{k},\uparrow}^\dagger c_{\mathbf{q}-\mathbf{k},\downarrow}^\dagger + \Delta^* c_{\mathbf{q}-\mathbf{k},\downarrow} c_{\mathbf{k},\uparrow}) - \frac{\Delta^2}{U}, \quad (1)$$

where the order parameter  $\Delta$  carries momentum  $\mathbf{q}$ . Using Bogoliubov transformation, it is easy to deduce the gap equation

via the self-consistency condition

$$\Delta \equiv -U \sum_{\mathbf{k}} \langle c_{\mathbf{k},\uparrow} c_{\mathbf{q}-\mathbf{k},\downarrow} \rangle, \quad (2)$$

which can be written as

$$\begin{aligned} 0 &= \frac{1}{U} + \sum_{\mathbf{k}} \left[ \frac{1 - f(E_{\mathbf{k}\mathbf{q},\uparrow}) - f(E_{\mathbf{k}\mathbf{q},\downarrow})}{2E_{\mathbf{k}\mathbf{q}}} \right] \\ &= \frac{1}{U} + \sum_{\mathbf{k}} \frac{1 - 2\bar{f}(E_{\mathbf{k}\mathbf{q}})}{2E_{\mathbf{k}\mathbf{q}}}, \end{aligned} \quad (3)$$

where  $E_{\mathbf{k}\mathbf{q}} = \sqrt{\xi_{\mathbf{k}\mathbf{q}}^2 + \Delta^2}$ ,  $E_{\mathbf{k}\mathbf{q},\uparrow} = E_{\mathbf{k}\mathbf{q}} + \zeta_{\mathbf{k}\mathbf{q}}$ ,  $E_{\mathbf{k}\mathbf{q},\downarrow} = E_{\mathbf{k}\mathbf{q}} - \zeta_{\mathbf{k}\mathbf{q}}$ ,  $\xi_{\mathbf{k}\mathbf{q}} = (\xi_{\mathbf{k},\uparrow} + \xi_{\mathbf{q}-\mathbf{k},\downarrow})/2$ ,  $\zeta_{\mathbf{k}\mathbf{q}} = (\xi_{\mathbf{k},\uparrow} - \xi_{\mathbf{q}-\mathbf{k},\downarrow})/2$ . We have defined the average

$$\bar{f}(x) \equiv [f(x + \zeta_{\mathbf{k}\mathbf{q}}) + f(x - \zeta_{\mathbf{k}\mathbf{q}})]/2, \quad (4)$$

where  $f(x)$  is the Fermi distribution function. The coupling constant  $U$  can be replaced by the dimensionless parameter,  $1/k_F a$ , via the Lippmann-Schwinger equation

$$\frac{1}{U} = \frac{m_r}{4\pi a} - \sum_{\mathbf{k}} \frac{1}{2\epsilon_{\mathbf{k}}}, \quad (5)$$

where  $a$  is the  $s$ -wave scattering length,  $m_r = 2m_{\uparrow}m_{\downarrow}/(m_{\uparrow} + m_{\downarrow})$  is twice the reduced mass, and  $\epsilon_{\mathbf{k}} = k^2/2m_r$ . Therefore the gap equation becomes

$$\frac{m_r}{4\pi a} = \sum_{\mathbf{k}} \left[ \frac{1}{2\epsilon_{\mathbf{k}}} - \frac{1 - 2\bar{f}(E_{\mathbf{k}\mathbf{q}})}{2E_{\mathbf{k}\mathbf{q}}} \right]. \quad (6)$$

The number density of each species is given by

$$n_{\sigma} = \sum_{\mathbf{k}} [f(E_{\mathbf{k}\mathbf{q},\sigma}) u_{\mathbf{k}\mathbf{q}}^2 + f(-E_{\mathbf{k}\mathbf{q},\bar{\sigma}}) v_{\mathbf{k}\mathbf{q}}^2], \quad (7)$$

where  $\bar{\sigma} = -\sigma$ , and the coherence factors  $u_{\mathbf{k}\mathbf{q}}^2 = (1 + \xi_{\mathbf{k}\mathbf{q}}/E_{\mathbf{k}\mathbf{q}})/2$ ,  $v_{\mathbf{k}\mathbf{q}}^2 = (1 - \xi_{\mathbf{k}\mathbf{q}}/E_{\mathbf{k}\mathbf{q}})/2$ . So the total number density  $n = n_{\uparrow} + n_{\downarrow}$  and the density difference  $\delta n \equiv n_{\uparrow} - n_{\downarrow}$  are given by

$$n = \sum_{\mathbf{k}} \left[ \left( 1 - \frac{\xi_{\mathbf{k}\mathbf{q}}}{E_{\mathbf{k}\mathbf{q}}} \right) + 2\bar{f}(E_{\mathbf{k}\mathbf{q}}) \frac{\xi_{\mathbf{k}\mathbf{q}}}{E_{\mathbf{k}\mathbf{q}}} \right], \quad (8)$$

$$\delta n = \sum_{\mathbf{k}} [f(E_{\mathbf{k}\mathbf{q},\uparrow}) - f(E_{\mathbf{k}\mathbf{q},\downarrow})]. \quad (9)$$

The thermodynamic potential  $\Omega_S$  is given by

$$\Omega_S = -\frac{\Delta^2}{U} + \sum_{\mathbf{k}} (\xi_{\mathbf{k}\mathbf{q}} - E_{\mathbf{k}\mathbf{q}}) - T \sum_{\mathbf{k},\sigma} \ln(1 + e^{-E_{\mathbf{k}\mathbf{q},\sigma}/T}). \quad (10)$$

Momentum  $\mathbf{q}$  is determined by minimizing  $\Omega_S$  at  $\mathbf{q}$ , i.e.,  $\frac{\partial \Omega_S}{\partial \mathbf{q}} = 0$ , which leads to

$$\sum_{\mathbf{k}} \left[ \frac{\mathbf{k}}{m_{\uparrow}} (n_{\mathbf{k}\mathbf{q}} + \delta n_{\mathbf{k}\mathbf{q}}) + \frac{\mathbf{q} - \mathbf{k}}{m_{\downarrow}} (n_{\mathbf{k}\mathbf{q}} - \delta n_{\mathbf{k}\mathbf{q}}) \right] = 0, \quad (11)$$

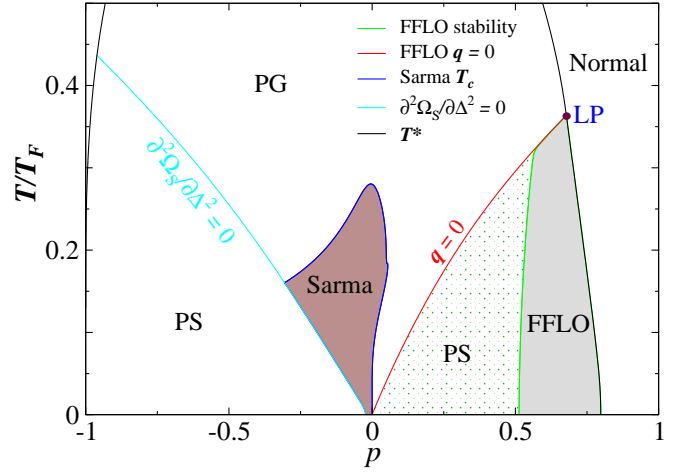


Figure 1. (Color online)  $T$ - $p$  phase diagram of a homogeneous  ${}^6\text{Li}$ - ${}^{40}\text{K}$  mixture at unitarity. Here “PG” and “PS” indicate pseudogapped normal state and phase separation, respectively, and LP labels a Lifshitz point. An FFLO superfluid (grey shaded) phase exists in the high  $p$  regime when  ${}^{40}\text{K}$  dominates, while it becomes unstable in the dotted region. A Sarma superfluid lives in the intermediate  $T$  and low  $p$  regime (brown shaded region).

where  $n_{\mathbf{k}\mathbf{q}}$  and  $\delta n_{\mathbf{k}\mathbf{q}}$  are given by the summands of Eqs. (8) and (9), respectively. Furthermore, the FFLO solutions are subject to the stability condition against phase separation (PS) [12, 28, 29],

$$\frac{\partial^2 \Omega_S}{\partial \Delta^2} \frac{\partial^2 \Omega_S}{\partial \mathbf{q}^2} - \left( \frac{\partial^2 \Omega_S}{\partial \Delta \partial \mathbf{q}} \right)^2 > 0. \quad (12)$$

This condition is equivalent to the positive definiteness of the particle number susceptibility matrix  $\{\partial n_{\sigma}/\partial \mu_{\sigma'}\}$  [12, 29]. For the Sarma phase (where  $\mathbf{q} = 0$ ), Eq. (12) is reduced to  $\partial^2 \Omega_S / \partial \Delta^2 > 0$  [29].

Equations (6), (8), (9) and (11) form a closed set of self-consistent equations, which can be used to solve for  $(\Delta, \mu_{\uparrow}, \mu_{\downarrow}, \mathbf{q})$  with various parameters  $1/k_F a$ ,  $p$ , and  $T$ , as well as the mass ratio  $m_{\uparrow}/m_{\downarrow}$ , and obtain the FFLO regions in phase diagrams. Since phase separation provides an alternative way to accommodate the excessive majority fermions, some of the mean-field solutions of the FFLO states are unstable against phase separation. Here we use the stability condition Eq. (12) to locate the phase boundary separating stable FFLO (or Sarma superfluid) phases and the PS phases. As a convention, we take the heavy (light) species to be spin up (down), and define Fermi momentum  $k_F = (3\pi^2 n)^{1/3}$ . To avoid an artificial jump across population imbalance  $p \equiv \delta n/n = 0$  in the phase diagrams, we take  $m = (m_{\uparrow} + m_{\downarrow})/2$  and define the Fermi temperature as  $T_F = k_F^2/2m$  as our energy unit.

Note that for the ( $\mathbf{q} = 0$ ) Sarma phases, we will use the pairing fluctuation theory described in Ref. [30] to determine the superfluid and pseudogap regions.

Figure 1 shows the calculated  $T$ - $p$  phase diagram for a homogeneous  ${}^6\text{Li}$ - ${}^{40}\text{K}$  mixture at unitarity. Pairing takes place below the pairing temperature  $T^*$  (black solid curve). A

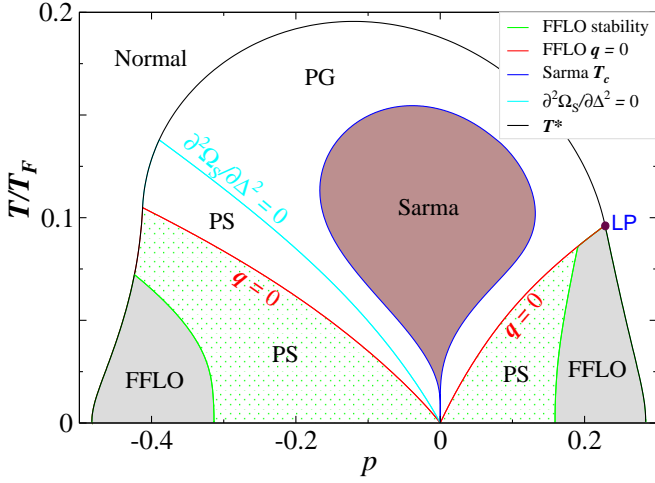


Figure 2. (Color online)  $T$ - $p$  phase diagram of a homogeneous  ${}^6\text{Li}$ - ${}^{40}\text{K}$  mixture at  $1/k_F a = -1$ , similar to Fig. 1. Here the FFLO phase (gray shaded regions) exists for both  $p > 0$  and  $p < 0$ .

mean-field FFLO solution exists to the lower right of the (red)  $\mathbf{q} = 0$  line. However, stable FFLO states exist only when  ${}^{40}\text{K}$  is the majority at relatively high  $p$  (in the grey shaded area). For lower  $p$ , FFLO states become unstable and phase separation takes place at low  $T$  (dotted region), whereas Sarma superfluid (brown area) and pseudogap states exist at intermediate  $T$ . The (green) line that separates the PS and the FFLO phases is given by the stability condition Eq. (12). When  ${}^6\text{Li}$  is the majority, i.e.,  $p < 0$ , phase separation dominates the low  $T$  region. Note here that, as we focus on the FFLO phases, we do not distinguish superfluid and pseudogap states in the PS regions. Further details regarding non-FFLO related phases can be found in Ref. [30].

Shown in Fig. 2 is the (near-)BCS counterpart of Fig. 1 at  $1/k_F a = -1$ , with much weaker pseudogap effects. Here we find stable FFLO phases for  $p < 0$  as well, when  ${}^6\text{Li}$  is the majority. This is different from Refs. [19, 20], which found no LO or supersolid states in the BCS regime for  $p < 0$ . The  $p > 0$  part is rather similar to the unitary case, except that everything moves to lower  $p$  and lower  $T$  due to weaker pairing strength. For  $p < 0$ , the  $\mathbf{q} = 0$  line splits the PS phase into two regions, representing unstable Sarma (upper) and FFLO (lower part) phases, respectively.

In both Figs. 1 and 2, we have found a Lifshitz point (as labeled “LP”) within the mean-field treatment, below which FFLO states emerge.

As the pairing strength grows, the Sarma phase becomes stabilized in a much larger region, especially for  $p < 0$  (not shown). However, the stable FFLO states are squeezed towards very low  $T$  and very high  $p \lesssim 1$ , and eventually disappear on the BEC side of the Feshbach resonance. Our result suggests that it is more promising to find FFLO phases in the unitary regime.

To ascertain the effect of a varying mass ratio  $m_\uparrow/m_\downarrow$ , we now focus on the stable FFLO superfluid phase for  $p > 0$  at

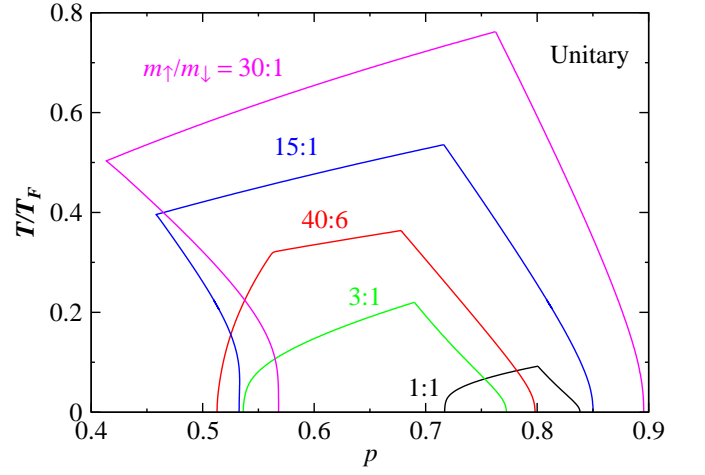


Figure 3. (Color online)  $T$ - $p$  phase diagram of stable FFLO superfluid in Fermi-Fermi mixtures with different mass ratios (as labeled) at unitarity. Large mass ratio enhances FFLO type of pairing.

unitarity and compute the phase diagram for a series of different mass ratios, as shown in Fig. 3. (The stable FFLO phase for  $p < 0$  quickly disappears when  $m_\uparrow/m_\downarrow \gtrsim 1.9$ ). Now that the mass ratio is changing, it is important to pick the right energy unit for meaningful comparison. In addition to the  $T_F$  used here, one may alternatively consider using  $m_r$  in the definition of  $T_F$ . The plot is shown in the supplemental Fig. S2. However, since  $m_r$  is an average based on the inverse mass, it puts more weight on the light species, which is more appropriate for the  $p < 0$  case. For the large  $p > 0$  case, where the heavy species dominates, we conclude that the present definition of  $T_F$  is more appropriate.

Figure 3 suggests that the FFLO  $T_c$  increases as the mass imbalance grows. At the same time, the phase space of stable FFLO superfluid also grows much larger as the mass ratio increases. In comparison with the mass balanced case, i.e.,  $m_\uparrow/m_\downarrow = 1$ , for  $m_\uparrow/m_\downarrow = 40 : 6$ , the enhancement of the FFLO  $T_c$  is about 3 times. For the  ${}^6\text{Li}$ - ${}^{173}\text{Yb}$  mixture [26, 27] which has a mass ratio near 30, the enhancement is about 7 times. Such great enhancement of  $T_c$  and enlarged phase space suggest that it is much easier to find experimentally the exotic FFLO superfluid with a large mass ratio. Note that one may also consider measuring  $T_c$  in units of the actual Fermi temperature of the heavy majority atoms,  $T_{F,\uparrow} = k_{F,\uparrow}^2/2m_\uparrow$ , which seems to be a natural choice for Ref. [18]. In this case, the enhancement of  $T_c$  by mass imbalance would be even more dramatic, being 7 and 16 times, respectively, as shown in the Supplemental Fig. S1.

Shown in Figs. 4 are the calculated  $p$ - $1/k_F a$  phase diagrams of a  ${}^6\text{Li}$ - ${}^{40}\text{K}$  mixture at  $T = 0$  for (a)  $p > 0$  and (b)  $p < 0$ , respectively. When  ${}^{40}\text{K}$  is the majority, Fig. 4(a) shows that a narrow (yellow shaded) region of stable FFLO superfluids persists from the BCS through the near-BEC regime, up to  $1/k_F a \approx 0.55$ , as  $p$  varies from 0 to 1. Apparently, in the near-BEC regime, the stable FFLO phase exists only at large  $p$ . On the other hand, when  ${}^6\text{Li}$  is the majority, the sta-

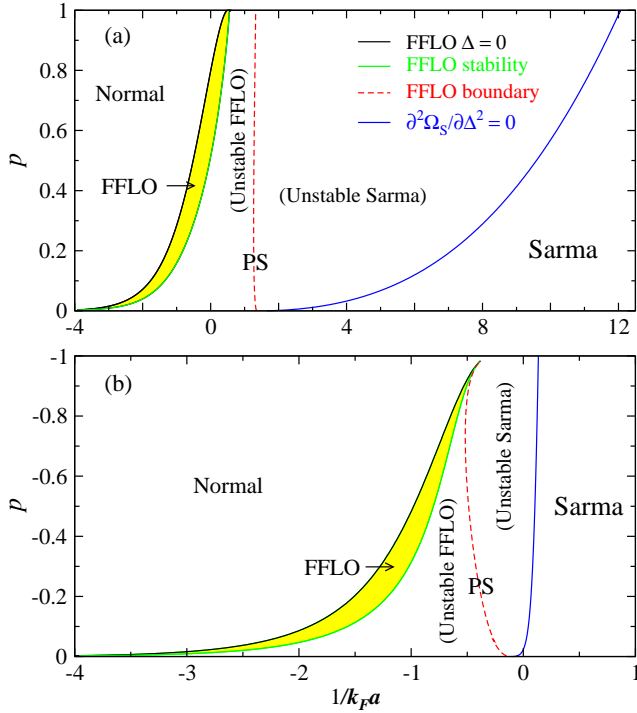


Figure 4. (Color online) Phase diagram of  ${}^6\text{Li}-{}^{40}\text{K}$  in the  $p-1/k_F a$  plane at  $T = 0$  for (a)  $p > 0$  and (b)  $p < 0$ . Stable FFLO phase lives in the narrow (yellow) shaded regions. Here “PS” labels phase separation (against unstable FFLO and Sarma superfluids), divided by the (red) dashed  $\mathbf{q} = 0$  line.

ble FFLO phase moves left completely to the BCS side, as shown in Fig. 4(b), in agreement with Figs. 1 and 2. In comparison with the equal-mass case [12], here the stable FFLO region for  $p > 0$  is slightly larger, while it becomes smaller for  $p < 0$ . Here “PS” in both figures labels the regions of FFLO and Sarma superfluids that are unstable against phase separations. In both cases, the FFLO  $\mathbf{q}$  vector increases from 0 in magnitude as  $|p|$  increases along the boundaries of the stable FFLO phase. The red dashed line separates from unstable FFLO and unstable Sarma regions.

More details about the behavior of  $\mathbf{q}$  as a function of interaction strength and population imbalance  $p$  are given in the Supplemental Information.

It is interesting to note that for  $p < 0$ , due to the left shift of the PS phase, the stable zero  $T$  Sarma superfluid phase has extended into the unitary regime ( $1/k_F a \gtrsim -0.1$ ) for small  $|p|$ , as can also be seen in Fig. 1, where the Sarma phase extends all the way down to  $T = 0$  at  $p \lesssim 0$ . This should be contrasted with the  $p > 0$  case and the equal mass case, where zero  $T$  Sarma superfluid can be found only when  $1/k_F a \gtrsim 1.5$  and  $1/k_F a \gtrsim 0.6$  [31], respectively.

Since a flat bottom or quasi-uniform trap has been realized experimentally [32], our homogeneous result may be directly applicable when such a trap is used. For a harmonic confining trap which causes inhomogeneity in terms of population imbalances [33–35], we take the study of the homogeneous case as a necessary first step. In addition, one may obtain exper-

imentally homogeneous result using a tomography technique [18]). In a trap, sandwich-like shell structures will emerge when  $p > 0$ , with superfluid or pseudogapped normal state in the middle shell [35]. Figure 1 suggests that the FFLO states may be found locally at low  $T$  near the shell interfaces where one may find suitable population imbalances.

Finally, we note that while more complex crystalline types of FFLO states are expected to have a lower energy and thus may be found within the PS phases in our phase diagrams. While one pair of  $\pm \mathbf{q}$  (i.e., the LO state) may lead to a lower energy, two pairs may further decrease the energy, and so on. It is not obvious where to stop the sequence. However, we expect this to cause only minor modifications in our results. Beyond-mean-field treatment may be more important than higher order crystalline types of pairing. For example, inclusion of particle-hole fluctuations may lead to a shift in the location of unitarity [36].

In summary, our results show that, in order to find the exotic FFLO states in a 3D Fermi gas, it is most promising to explore Fermi-Fermi mixtures with a large mass ratio in the unitary regime, where one expects to see a relatively large phase space volume and a greatly enhanced superfluid transition temperature when the heavy species is the majority. While we have focused on the one-plane-wave FFLO, i.e., the FF case, such enhancement is present for the LO phase as well, which has a comparable or lower energy. These FFLO states may be detected via collective modes [37], vortices [38], direct imaging [39], rf spectroscopy [40], triplet pair correlations [41], and, most directly, by measuring the pair momentum distribution which should exhibit a peak at a finite  $\mathbf{q}$ . Experimentally, the  $T \ll T_{F,\uparrow}$  regime has now been accessible for  ${}^6\text{Li}-{}^{40}\text{K}$  [18]. With the recent report of  $T \simeq 0.3T_{F,\uparrow}$  [27], it is hopeful that lower  $T$  regime can be accessed for  ${}^6\text{Li}-{}^{173}\text{Yb}$  as well in the near future. These experimental progress makes it promising to observe the exotic FFLO states if they do exist.

This work is supported by NSF of China (Grant No. 11274267), the National Basic Research Program of China (Grants No. 2011CB921303 and No. 2012CB927404), NSF of Zhejiang Province of China (Grant No. LZ13A040001).

\* Corresponding author: qchen@zju.edu.cn

- [1] Q. J. Chen, J. Stajic, S. N. Tan, and K. Levin, Phys. Rep. **412**, 1 (2005).
- [2] I. Bloch, J. Dalibard, and W. Zwerger, Rev. Mod. Phys. **80**, 885 (2008).
- [3] P. Fulde and R. A. Ferrell, Phys. Rev. **135**, A550 (1964).
- [4] A. I. Larkin and Y. N. Ovchinnikov, Zh. Eksp. Teor. Fiz. **47**, 1136 (1964) [Sov. Phys. JETP **20**, 762 (1965)].
- [5] R. Casalbuoni and G. Nardulli, Rev. Mod. Phys. **76**, 263 (2004).
- [6] A. Bianchi, R. Movshovich, N. Oeschler, P. Gegenwart, F. Steglich, J. D. Thompson, P. G. Pagliuso, and J. L. Sarrao, Phys. Rev. Lett. **89**, 137002 (2002).
- [7] A. G. Lebed and S. Wu, Phys. Rev. B **82**, 172504 (2010).
- [8] A. B. Vorontsov, J. A. Sauls, and M. J. Graf, Phys. Rev. B **72**,

- 184501 (2005).
- A. M. Berridge, A. G. Green, S. A. Grigera, and B. D. Simons, *Phys. Rev. Lett.* **102**, 136404 (2009).
- K. Cho, H. Kim, M. A. Tanatar, Y. J. Song, Y. S. Kwon, W. A. Coniglio, C. C. Agosta, A. Gurevich, and R. Prozorov, *Phys. Rev. B* **83**, 060502R (2011).
- [9] H. Mütther and A. Sedrakian, *Phys. Rev. C* **67**, 015802 (2003).
- [10] M. Alford, J. Bowers, and K. Rajagopal, *Phys. Rev. D* **63**, 074016 (2001).
- [11] A. Sedrakian, J. Mur-Petit, A. Polls, and H. Mütther, *Phys. Rev. A* **72**, 013613 (2005).
- Y.-A. Liao, A. S. C. Rittner, T. Paprota, W. Li, G. B. Partridge, R. G. Hulet, S. K. Baur, and E. J. Mueller, *Nature* **467**, 567 (2010).
- L. Radzihovsky and D. E. Sheehy, *Rep. Prog. Phys.* **73**, 076501 (2010).
- [12] Y. He, C.-C. Chien, Q. J. Chen, and K. Levin, *Phys. Rev. A* **75**, 021602 (2007).
- D. E. Sheehy and L. Radzihovsky, *Phys. Rev. Lett.* **96**, 060401 (2006).
- H. Hu and X.-J. Liu, *Phys. Rev. A* **73**, 051603 (2006).
- [13] L. He, M. Jin, and P. Zhuang, *Phys. Rev. B* **74**, 214516 (2006).
- R. Combescot and C. Mora, *Phys. Rev. B* **71**, 144517 (2005).
- N. Yoshida and S.-K. Yip, *Phys. Rev. A* **75**, 063601 (2007).
- [14] K. Machida, T. Mizushima, and M. Ichioka, *Phys. Rev. Lett.* **97**, 120407 (2006).
- [15] W. Zhang and L.-M. Duan, *Phys. Rev. A* **76**, 042710 (2007).
- [16] J. Kinnunen, L. M. Jensen, and P. Törmä, *Phys. Rev. Lett.* **96**, 110403 (2006).
- [17] M. W. Zwierlein, A. Schirotzek, C. H. Schunck, and W. Ketterle, *Science* **311**, 492 (2006).
- G. B. Partridge, W. Li, R. I. Kamar, Y. A. Liao, and R. G. Hulet, *Science* **311**, 503 (2006).
- [18] Y.-I. Shin, C. H. Schunck, A. Schirotzek, and W. Ketterle, *Nature* **451**, 689 (2008).
- [19] K. B. Gubbels, J. E. Baarsma, and H. T. C. Stoof, *Phys. Rev. Lett.* **103**, 195301 (2009).
- J. E. Baarsma, K. B. Gubbels, and H. T. C. Stoof, *Phys. Rev. A* **82**, 013624 (2010).
- [20] J. E. Baarsma and H. T. C. Stoof, *Phys. Rev. A* **87**, 063612 (2013).
- [21] Z. Zheng, M. Gong, X. Zou, C. Zhang, and G. Guo, *Phys. Rev. A* **87**, 031602 (2013).
- X.-J. Liu and H. Hu, *Phys. Rev. A* **87**, 051608(R) (2013).
- [22] X.-F. Zhou, G.-C. Guo, W. Zhang, and W. Yi, *Phys. Rev. A* **87**, 063606 (2013).
- F. Wu, G.-C. Guo, W. Zhang, and W. Yi, *Phys. Rev. Lett.* **110**, 110401 (2013).
- L. Dong, L. Jiang, and H. Pu, *New J. Phys.* **15**, 075014 (2013).
- H. Hu and X.-J. Liu, *New J. Phys.* **15**, 093037 (2013).
- M. Iskin, *Phys. Rev. A* **88**, 013631 (2013).
- [23] Z. Cai, Y. Wang, and C. Wu, *Phys. Rev. A* **83**, 063621 (2011).
- V. V. Franca, D. Hördlein, and A. Buchleitner, *Phys. Rev. A* **86**, 033622 (2012).
- R. Mendoza, M. Fortes, M. A. Solís, and Z. Koinov, *Phys. Rev. A* **88**, 033606 (2013).
- Y. Okawauchi and A. Koga, *J. Phys. Soc. Jpn.* **81**, 074001 (2012).
- D.-H. Kim and P. Törmä, *Phys. Rev. B* **85**, 180508(R) (2012).
- A.-H. Chen and G. Xianlong, *Phys. Rev. B* **85**, 134203 (2012).
- [24] Here the supersolid state is just the LO state.
- [25] E. Wille, F. M. Spiegelhalder, G. Kerner, D. Naik, A. Trenkwalder, G. Hendl, F. Schreck, R. Grimm, T. G. Tiecke, J. T. M. Walraven, et al., *Phys. Rev. Lett.* **100**, 053201 (2008).
- D. Naik, A. Trenkwalder, C. Kohstall, F. Spiegelhalder, M. Zaccanti, G. Hendl, F. Schreck, R. Grimm, T. Hanna, and P. Julienne, *Eur. Phys. J. D* **65**, 55 (2011).
- M. Taglieber, A.-C. Voigt, T. Aoki, T. W. Hänsch, and K. Dieckmann, *Phys. Rev. Lett.* **100**, 010401 (2008).
- [26] T. Fukuhara, Y. Takasu, M. Kumakura, and Y. Takahashi, *Phys. Rev. Lett.* **98**, 030401 (2007).
- [27] A. H. Hansen, A. Y. Khramov, W. H. Dowd, A. O. Jamison, B. Plotkin-Swing, R. J. Roy, and S. Gupta, *Phys. Rev. A* **87**, 013615 (2013).
- [28] C.-H. Pao, S.-T. Wu, and S.-K. Yip, *Phys. Rev. B* **73**, 132506 (2006).
- [29] Q. J. Chen, Y. He, C.-C. Chien, and K. Levin, *Phys. Rev. A* **74**, 063603 (2006).
- [30] H. Guo, C.-C. Chien, Q. J. Chen, Y. He, and K. Levin, *Phys. Rev. A* **80**, 011601 (2009).
- [31] C. C. Chien, Q. J. Chen, Y. He, and K. Levin, *Phys. Rev. Lett.* **97**, 090402 (2006).
- [32] A. L. Gaunt, T. F. Schmidutz, I. Gotlibovych, R. P. Smith, and Z. Hadzibabic, *Phys. Rev. Lett.* **110**, 200406 (2013).
- [33] C. C. Chien, Q. J. Chen, Y. He, and K. Levin, *Phys. Rev. Lett.* **98**, 110404 (2007).
- [34] C.-H. Pao, S.-T. Wu, and S.-K. Yip, *Phys. Rev. A* **76**, 053621 (2007).
- [35] J. B. Wang, H. Guo, and Q. J. Chen, *Phys. Rev. A* **87**, 041601 (2013).
- [36] Q. J. Chen, *Sci. Rep.* **6**, 25772 (2016).
- [37] J. M. Edge and N. Cooper, *Phys. Rev. Lett.* **103**, 065301 (2009).
- [38] D. Agterberg, Z. Zheng, and S. Mukherjee, *Phys. Rev. Lett.* **100**, 017001 (2008).
- [39] T. Mizushima, K. Machida, and M. Ichioka, *Phys. Rev. Lett.* **94**, 060404 (2005).
- [40] M. R. Bakhtiari, M. J. Leskinen, and P. Torma, *Phys. Rev. Lett.* **101**, 120404 (2008).
- [41] I. Zapata, F. Sols, and E. Demler, *Phys. Rev. Lett.* **109**, 155304 (2012).